

# Emerging measures of local geometry in trabecular bone: case studies of intertrabecular angle distributions

A. A. Felder<sup>1</sup>, M. Doube<sup>1</sup>

<sup>1</sup>Royal Veterinary College, 4 Royal College Street, UK

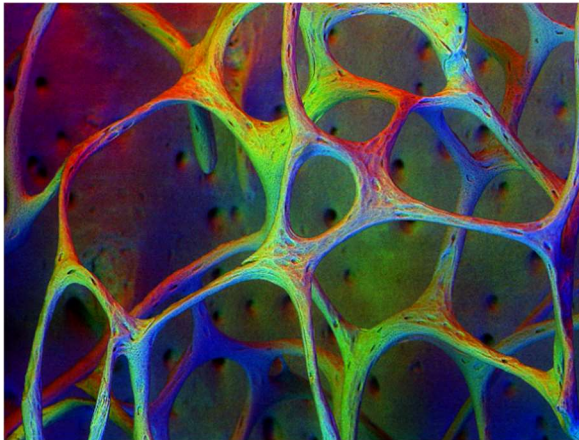


Figure 1: Backscattered electron scanning-electron micrograph of trabecular bone. Image credit: Duncan Bassett, Alan Boyde and Graham Williams via Bone Research Society website.

## Aims

Trabecular bone is the irregular porous solid found in the ends of many long bones and within vertebrae (Figure 1). The components of trabecular bone ("trabeculae", latin for "little beams") are usually described to be rod-like or plate-like in shape, but various intermediate forms exist<sup>1</sup>. Trabecular bone functions to redistribute the loads exerted on the bone organ, adding mechanical strength. It has long been hypothesized that trabeculae follow the stress trajectories of a prevalent loading state ("trajectorial theory"), with the necessary consequence of arranging at right angles to each other (Figure 2) and nodes having six connections. Evidence for this is based mostly on two-dimensional radiographs of the heel bones of artiodactyls (deer and sheep)<sup>2</sup> and small marsupials<sup>3</sup>. This century-old view, while not accepted whole-sale, has often been vaguely referred to or ignored, but rarely challenged until recently<sup>4,5</sup>.

Reznikov and colleagues<sup>6</sup> proposed a novel way to measure the distribution of valences (number of outgoing trabeculae from a junction) and angles between (rod-like) trabeculae in three dimensions, the intertrabecular angle (ITA) algorithm. ITA is based on a topology-preserving thinning algorithm, the skeletonization, of binary images derived from three-dimensional images of bone (obtained e.g. by X-ray microtomography). The skeletonized binary image is a set of voxel-thin curves representing the original image foreground. In ITA, this set of curves is further simplified to consist of straight lines connecting nodes. Connections shorter than a user-defined cut-off value (usually taken to be the average trabecular thickness) are

simplified to a node (Figure 3). Angle and valence distributions of the resulting nodes are then calculated. In previously studied bones<sup>6,7,8</sup>, ITA suggests diverse samples of trabecular bone display strikingly similar ITA patterns, consisting of predominantly 3-connected and 4-connected nodes that arrange at maximal angles to each other (Figure 4).

The aims of the present study were (1) to validate a re-implementation of ITA as an ImageJ2<sup>9</sup> plug-in, (2) study the effect of the image resolution on ITA results and (3) measure ITA distributions in trabecular bone from mammalian femora of vastly different size.

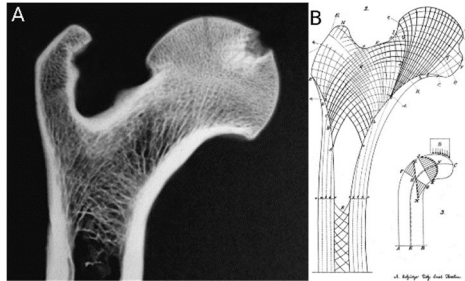


Figure 2. (A) Radiograph of chimpanzee femur section: while some trabeculae may be at right angles, some are clearly not. Also, depth information is missing from this kind of image. (B) Wolff's original illustration of the trajectorial theory. Reused with kind permission from reference 4.

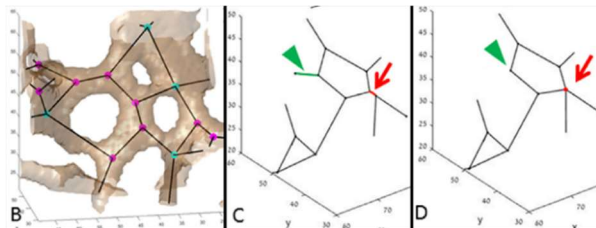


Figure 3. Illustration of the ITA algorithm. The result of a skeletonization algorithm is simplified into a graph-like network (B), Short edges (C) are further culled or replaced by a central node. Image adapted with kind permission from reference 6.

## Method

ITA was re-implemented as an ImageJ2 command and distributed as part of the development version of BoneJ<sup>10</sup>, a collection of skeletal biology-related image analysis algorithms. On an implementation level, ITA was split into three Ops that simplify the skeletonization, sort the nodes by their valence and compute the angles around a node, respectively. All results reported here were obtained using the the ImageJ2 version of ITA.

ITA was run on a lattice consisting of rhombic dodecahedral cells containing a frame, with known valence proportions (50% four-connected, 25% six-connected, 25% 14-connected nodes) and angle distributions (109.5 degrees for four connected nodes, mostly 90 degrees for six-connected nodes), to validate the ITA implementation.

An image of bovine trabecular bone was used to elucidate the effect of resampling on ITA. Resampling factors of 1,2,4,8,16, and 32 were used, resulting in voxel size ranging from 8.2  $\mu\text{m}$  by 8.2  $\mu\text{m}$  by 8.2  $\mu\text{m}$  to 262  $\mu\text{m}$  by 262  $\mu\text{m}$  by 262  $\mu\text{m}$ . Figure 6 shows the effect of resampling on the skeletonization.

Finally, ITA was computed for a series of trabecular bone samples taken from the femora of 33 mammalian species available from a previous study<sup>11</sup>. X-ray microtomographs were binarized and resampled in order for the average trabecular thickness to match  $\sim 5$  pixels, which corresponds to the resolution of previous studies<sup>6,7,8</sup>.

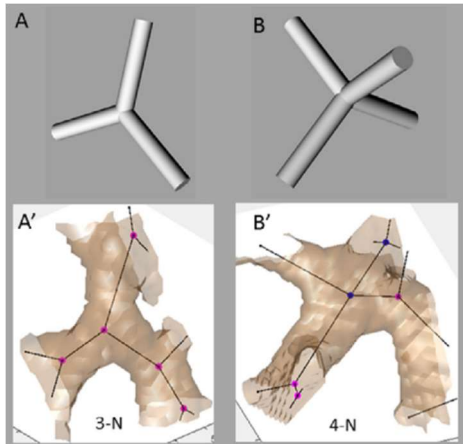


Figure 4 (below). Previous studies<sup>5,6,7</sup> suggest most nodes in human femora are 3-connected ( $\sim 70\%$ ) or 4-connected ( $\sim 25\%$ ). The mean of the broad angle distribution (st. dev.  $\sim 30^\circ$ ) is located close to  $120^\circ$  (3N) and  $109.5^\circ$  (4N), suggesting a tendency towards maximal angles. Image adapted with kind permission from reference 6.

**Results**

Validation study shows the correct, expected distributions (see Methods), which are similar to the ones obtained on the same geometry in a previous study<sup>8</sup>.

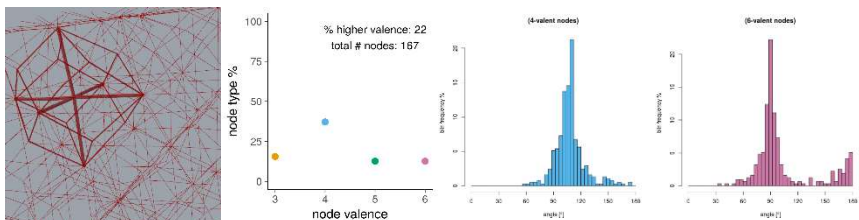


Figure 5: From left to right: Skeletonization of a lattice formed of rhombic dodecahedral cells (cell boundary highlighted with medium thick line) containing orthogonal frames (fully thick line); Valence distributions of this lattice; angle distribution around 4-connected nodes; angle distributions around 6-connected nodes.

*Effect of resampling on ITA results*

Figure 6 shows that the skeletonization algorithm, on which ITA is intrinsically dependent, gives different outputs at varying resolutions of the input. This results in vastly different values for the angle and valence distributions of the same sample at high and low resolutions. At high resolution, this is likely a consequence of intratrabecular feature such as blood vessels and osteocyte lacunae affecting the skeletonization. At low resolutions, the binarized image is too noisy to represent the original geometry adequately. Where the resolution is similar to previous studies (resampling factor 8) the patterns (prevalence of 3-connected nodes, larger mean and median angles in three-connected nodes compared to four-connected nodes) agree with previous studies<sup>6,7,8</sup>, but the values for proportion of 3-connected nodes are lower and angle distributions are not as close to the hypothesized maximal spanning.

#### *Effect of animal size on ITA results*

Despite vast differences in size (and locomotor mode, phylogenetic background and habitat), ITA results suggest that trabeculae arrange according to the same geometric pattern throughout mammalian species (Figure 7). As in the resampling study, patterns, but not always values, match previous studies. In particular, there is a high variation in the proportion of 3-connected nodes.

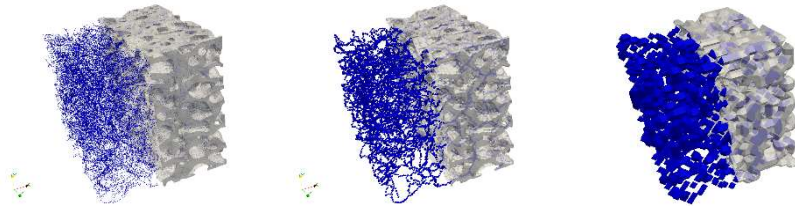


Figure 6: Evolution of number of attendees and submitted abstracts. Output (blue) of the skeletonization of a binarized image (grey) of bovine trabecular bone of varying resolution. (A) No resampling, voxel size 8.2  $\mu\text{m}$  by 8.2  $\mu\text{m}$  by 8.2  $\mu\text{m}$ . (B) Resampling factor 8; voxel size 65.6  $\mu\text{m}$  by 65.6  $\mu\text{m}$  by 65.6  $\mu\text{m}$  (similar to previous studies) (C) Resampling factor 32; voxel size 262  $\mu\text{m}$  by 262  $\mu\text{m}$  by 262  $\mu\text{m}$ .

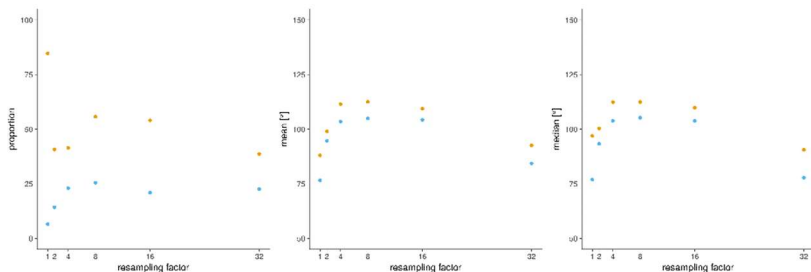


Figure 7: Various resampling factors give different ITA results (f.l.t.r valence proportions, mean angle, median angle). At higher resolutions, the skeletonization picks up various pores within the bone matrix, while at low resolutions it does not meaningfully represent the original image anymore (See also Figure 5).

**Conclusion**

The ImageJ2 implementation of ITA is able to measure “ground truth” angles in a validation lattice correctly. However, both in the resampling and the animal size study, ITA patterns are similar, but ITA values are different to previous studies<sup>6,7,8</sup>. There could be several explanations for this.

One possibility are methodological differences. Samples examined here contain less trabeculae than in previous studies. Short edges were detected differently compared to previous publications to avoid a dependency on the order in which edges were traversed. This favours the creation of nodes of higher valence in the simplification step.

The samples here were also not necessarily chosen to contain rod-like trabeculae. In “sandwich” configurations (plates connected by orthogonal rods), this could lead to spurious 3-connected nodes arrange in a maximal spanning way (Figure 9).

ITA provides a novel way to measure angle and valence distributions of trabecular bone in three dimensions, challenging outdated views and giving more insight into structure-function relationships of bone tissue. The results show that more validation study of ITA are needed and highlight the importance of a meaningful binarization and skeletonization. An improved ITA algorithm could be obtained by combining the detection of nodes with measures of local shape, e.g Ellipsoid Factor<sup>1</sup>. This could possibly help quantify the meaningfulness of the skeletonization or to distinguish “true” from artefactual trabecular junctions. Thanks to the re-implementation of ITA, this can now be done more easily in the future.

ITA could also be used in other fields to determine the angle arrangement of synthetic and natural cellular solids at various scales, provided the arrangement is suited to representation by a skeletonization.

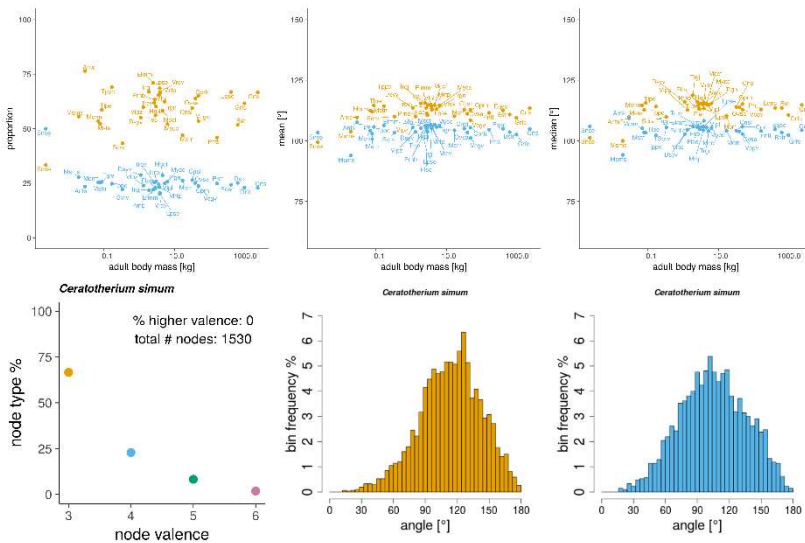


Figure 8. Top row f. l. t. r. valence proportions, mean and median angles for trabecular bone from mammalian femora of vastly different size. Orange data points for 3-connected nodes, blue data points for 4-connected nodes. Bottom row f. l. t. r. Valence and angle distribution of trabecular bone of a rhinoceros.



Figure 9. An artificial “sandwich” image (three horizontal plates connected by orthogonal rods, light blue on the left) leads to the creation of artefactual 3-connected “trabecular” junctions with maximal spanning angles.

### Acknowledgements

An X-ray microtomograph of the validation lattice was kindly provided by Natalie Reznikov (McGill University). AF thanks Natalie Reznikov and Crispin Wiles (Imperial College London) for helpful discussions about ITA. AF acknowledges support by an RVC PhD studentship and BBSRC post-doctoral research grant (BB/P006167/1). RD is supported by the Wellcome Trust.

### References:

1. Doube, M. “The Ellipsoid Factor for Quantification of Rods, Plates, and Intermediate Forms in 3D Geometries”, *Front. Endocrinol.* 6, (2015).
2. Lanyon, L. E. “Experimental support for the trajectorial theory of bone structure”, *Bone & Joint Journal* 56, 160–166 (1974)
3. Biewener, A. A., Fazzalari, N. L., Koniczynski, D. D. & Baudinette, R. V. “Adaptive changes in trabecular architecture in relation to functional strain patterns and disuse.” *Bone* 19, 1–8 (1996).
4. Skedros, J. G. & Baucom, S. L. “Mathematical analysis of trabecular ‘trajectories’ in apparent trajectorial structures: The unfortunate historical emphasis on the human proximal femur.” *Journal of Theoretical Biology* 244, 15–45 (2007).
5. Hammer, A. “The paradox of Wolff’s theories.” *Irish Journal of Medical Science* 184, 13–22 (2015).
6. Reznikov, N. et al. “Inter-trabecular angle: A parameter of trabecular bone architecture in the human proximal femur that reveals underlying topological motifs.” *Acta Biomaterialia* 44, 65–72 (2016).
7. Reznikov, N. et al. “Functional adaptation of the calcaneus in historical foot binding.” *J Bone Miner Res* (2017).
8. Ben-Zvi, Y., Reznikov, N., Shahar, R. & Weiner, S. “3D Architecture of Trabecular Bone in the Pig Mandible and Femur: Inter-Trabecular Angle Distributions.” *Front. Mater.* 4, (2017).
9. Rueden, C. T. et al. “ImageJ2: ImageJ for the next generation of scientific image data.” *arXiv:1701.05940* (2017).
10. Doube, M. et al. BoneJ: Free and extensible bone image analysis in ImageJ. *Bone* 47, 1076–1079 (2010).
11. Doube, M., Klosowski, M. M., Wiktorowicz-Conroy, A. M., Hutchinson, J. R. & Shefelbine, S. J. “Trabecular bone scales allometrically in mammals and birds.” *Proceedings of the Royal Society B: Biological Sciences* 278, 3067–3073 (2011).